PROCEEDINGS, 13th Indonesia International GEOTHERMAL Convention & Exhibition 2013
Assembly Hall - Jakarta Convention Center Indonesia, June 12 – 14, 2013

AIRBORNE MAGNETIC DATA FOR LITHOLOGIC MAPPING USING EDGE DETECTION METHOD

Husin Setia Nugraha[*], Emmanuel J. M. Carranza[**], and Mark Van Der Meijde[***]

[*)] Directorate for Geothermal, MEMR
Pegangsaan Timur 1A, Jakarta
e-mail: husin_setia_n@yahoo.com

[**)] School of Earth and Environmental Science
James Cook University
Townsville, Qld 4811 - Australia

[***)] Faculty of Geo-Information Science and Earth Observation (ITC)
University of Twente
Hengelosestraat 99 Enschede- The Netherlands

ABSTRACT

Two edge detection methods, Rotation-variant Template Matching (RTM) and Clustering-based for Edge Detection (CED), were been used to indicate lithology boundaries in analyzing airborne magnetic data. Reduce to pole (RTP) and analytic signal (AS) transformation were been applied in data preparation. RTP and AS transformation to data at latitude more than 50° produced similar results in application of these edge detection methods. The edge detection method such as RTM and CED, could be applied to airborne magnetic data in order to help lithologic mapping by distinguishing intrusive complex rocks to surrounding rocks.

Keywords : Airborne Magnetic, British Columbia Canada; Rotation-variant Template Matching (RTM); Clustering-based for Edge Detection (CED)

INTRODUCTION

This paper tried to use edge detection method to indicate lithology boundaries. Two techniques, Rotation-variant Template Matching (RTM) and Clustering-based for Edge Detection (CED), were performed. Before application of the techniques, two common transformations in analysing magnetic data, reduce to pole (RTP) and analytic signal (AS) transformation, were applied in data preparation. The results were used to interpret lithology boundaries. The method was being applied to airborne magnetic data.

Study Area

The study area is situated at regional district of Bulkley-Nechako. The district is located in Northern-Central of British Columbia province (*figure 1*). The dominant landform of this regional district is the Nechako plateau. The areas consist of Bulkley Valley, the northern part of the Nechako District, and the Omineca District, including portions of the Hazelton Mountains and Omineca Mountains in the west and north of the regional district, respectively (http://en.wikipedia.org/wiki/Regional_District_of_Bulkley-Nechako). The study area bounded by geographic coordinates (372750 mW, 6095500 mN) and (423500 mW, 6134500 mN) and covers an area of ~ 2,000 km^2.

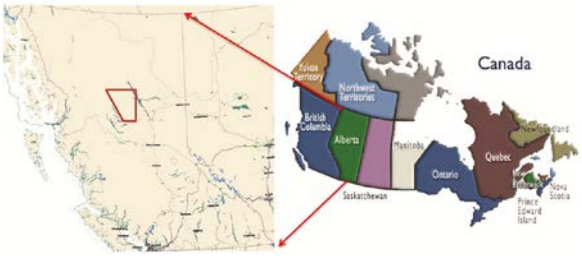


Figure 1 Map showing location of study area.

Geology

The area is dominantly underlain by quesnel terrane or quesnelia. Two group rocks form the terrane, the Takla group at northern part and the Nicola group at southern part. The terrane is intruded by northwest-elongate hogem batholiths. The Takla group consists of a sedimentary unit at lower late Triassic in age.

The group is overlain by volcanic, pyroclastic, and epiclastic rocks; and intruded by early a Jurassic pluton. Augite phyric rocks are dominant with plagioclase and hornblende (Nelson et al.,1992; Nelson, 1991). Takla group volcanics contain rocks that are unusually potassium rich and alkalic in their major element chemistry (Delong, 1996).
Nelson (1991) divided Takla Group into four interfingering formations, the Rainbow Creek, Inzana Lake, Witch Lake and Chuchi Lake formations. In stratigraphy, Rainbow Creek is the lowest unit overlain by Inzana Lake, Witch Lake, Chuci Lake formation, in upward sequence. The Rainbow Creek Formation is comprised of dark grey to black slate or phyllites with interbeded quart-rich siltstone and sandstone. The Inzana Lake Formation consists of epiclastic and sedimentary rocks with minor pyroclastic rocks. The Witch Lake Formation is dominated by an augite porphyry suite which is produced from explosive intermediate volcanism. Chuchi Lake Formation is made up of volcanic rocks with andesitic to latite-andesite composition. The phenocryst assemblage is dominated by plagioclase with variable amounts of augite and hornblende (Delong, 1996; Nelson, 1991).

Figure 2 is simplified lithologic map which was used for validation in. The lithologic units were divided regarding to age group. For sedimentary rocks, the lithological units were divided into two lithological units based on the age (Jurassic to quaternary and Triassic to Jurassic). Small lithological units such as ultramafic rocks and metamorphic rocks were diffused into lithological unit where the lithological units lie within. Intrusive rocks comprise two formations which are Chuchi Syenite and Klawli Pluton Formation whereas other two formations, Chuchi Lake Succession Formation and Witch Lake Formation exist in Volcanic Rocks.

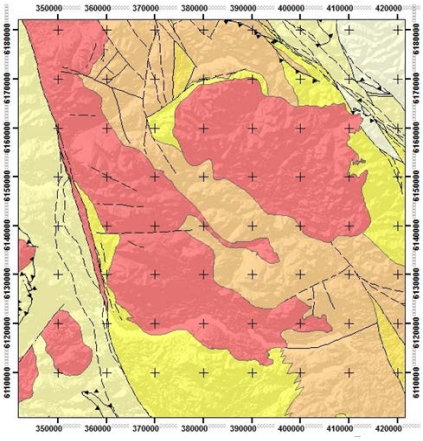


Figure 2 Simplified existing geological map (Modified from Massey et al., 2005a, b, c; Massey et al., 2005d)

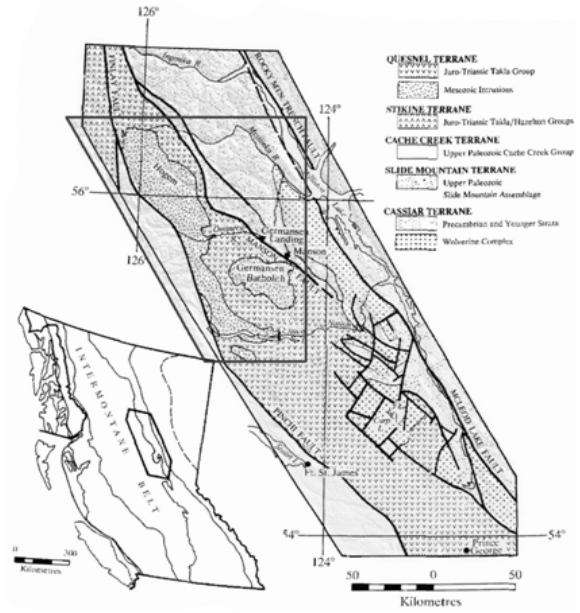


Figure 3 Regional structure of study area (Nelson, 1991)

The area lies between two regional-scale northwest-trending systems (*figure 3*). The Pinchi fault lies at the western part and the Manson, McLeod, and at eastern part is the Northern Rocky Mountain Trench Fault (Nelson et al., 1992; Nelson, 1991).

Datasets

Airborne magnetic data is obtained from the Canadian Aeromagnetic Database maintained by the Geological Survey of Canada. Compiling data of residual total magnetic intensity were downloaded from the Geological Survey of Canada website (Natural Resources Canada, 2010). The data were available in grid form with 200-m size with coordinate system in WGS 1984 UTM zone 10 N and datum of WGS 1984 datum. Residual total magnetic is obtained from the subtraction of observed total field by International Geomagnetic Reference Field (IGRF) model (Natural Resources Canada, 2010). Then the data were resampled into 500 m grid and subset into study area.

The 200 m grid data are derived from airborne magnetic surveys that were conducted by the Geological Survey of Canada. In the surveys, the flight-line orientations were designed to perpendicular to the regional strike in constant line spacing. Most the data acquired by the survey with 305 m of mean terrain clearance with 800 m in flight line spacing. For the areas where the deep sedimentary basins are dominant, the flight-line spacing was increased up to 1.6 km (Natural Resources Canada, 2010).

METHODOLOGY

Two techniques of edge detection were applied to airborne magnetic in order to identify lithology boundaries. Rotation-variant Template Matching (RTM) algorithm developed by Van der Werff et al. (2007) and Clustering-based for Edge Detection (CED) algorithm developed by Dinh et al. (2009) were tried to be applied to airborne magnetic data with some preparation processes before the application as can be seen in the flow chart (*figure 4*). RTM algorithm was applied to subtraction image whereas CED was applied to horizontal derivatives image. Template matching technique was applied using ENVI software with ESA tools extension whereas *k-means* clustering, the last part of CED algorithm, was applied using *R* statistic software with *stats* package (R Core Team, 2013).

Preparation

For comparison, two linear transformations, reduce to pole (RTP) and analytic signal (AS), were employed to prepare airborne magnetic data before the application of edge detection techniques. As it is shown in *figure 4*, after RTP or AS transformation, upward continuation (UC) was applied to each image. The last process in preparation stage is raster/grid subtraction of RTP and AS image by their UC. The results of their subtraction are so-called RTP subtraction (RTPS) and AS subtraction images (ASS), respectively.

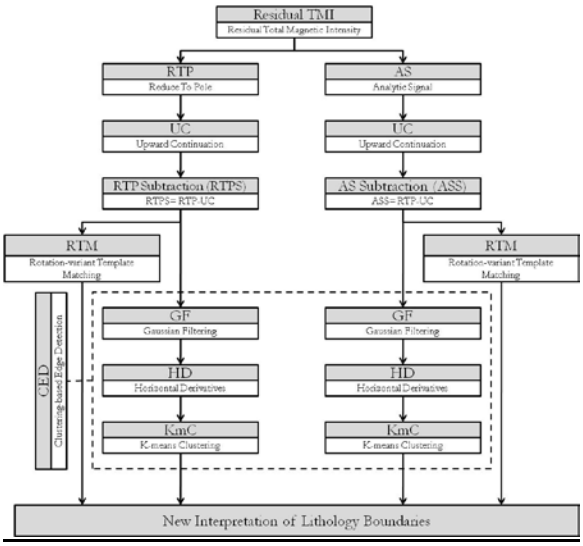


Figure 4 Flow chart of the methodology with two different transformations, RTP and AS; and techniques, RTM and CED.

Milligan and Gunn (1997) defined reduce to pole (RTP) as the process to convert the magnetic field form a magnetic latitude to the field at a magnetic pole, where inducing field is vertical. At magnetic latitude, magnetic anomalies due to induction have asymmetric form (skewed form) related to their sources, but when the inducing is vertical the induced anomalies are directly over their sources as shown in *figure 5* (Blakely, 1996).

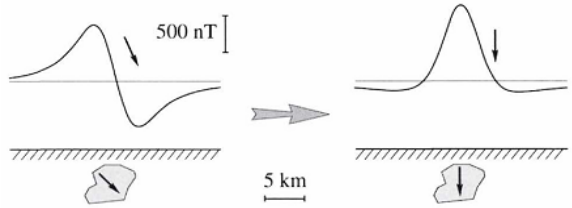


Figure 5 A magnetic anomaly profile and its relation to geological features, before and after being reduced to the pole (Blakely, 1996).

Reduce to pole transformation was applied to the airborne magnetic data using *Oasis Montaj 7.2*. The formula is used by *Oasis Montaj 7.2* to reduce the pole is as follow (Whitehead and Musselman, 2010):

$$L(\theta) = \frac{[sin(I) - i.cos(I).cos(D-\theta)]^2}{[sin^2(I_a) + cos^2(I_a).cos^2(D-\theta)].[sin^2(I) + cos^2(I).cos^2(D-\theta)]}$$

$$\text{if } (|I_a| < |I|),\ I_a = I \quad \text{.....Equation 1}$$

where:

I = geomagnetic inclination

I_a = inclination for magnitude correction (never less than I)

D = geomagnetic declination

with the *sin(I)* term and *i.cos(D-θ)* term as a magnitude and a phase component of reduction to the pole, respectively. The default value for I_a is ±20 degrees, if $|I_a|$ is specified to be less than $|I_a|$, it is set to I (Whitehead and Musselman, 2010).

Limitations of using RTP transformation are its application in low latitude areas and its assumption that all bodies are magnetized by induction. In the situation where the latitude is less than 15° (near equator) the transformation become unstable (Milligan and Gunn, 1997). When *equation 1* is applied in the areas with low latitude, the equation will amplify the total field anomaly and the noise. Asymmetric shape with the anomalies and more elongated in the direction of the declination will be produced (Blakely, 1996). The basic assumption is that all bodies are magnetized by induction but not in the real cases. However, according to Milligan and Gunn (1997), significance remnant magnetization is rarely to appear. Thus this limitation can be ignored.

Analytic Signal (AS)

Analytic signal is a linear combination of first derivates magnetic anomaly in horizontal and vertical direction as describing in *equation 2* from (Roest et al., 1992). The analytic signal has a form over causative bodies that depend on the locations of the bodies but not on their directions of magnetization. This means that all bodies with the same geometry have same analytic signal. The analytic signal peaks over the edges of source bodies of positive and negative anomalies and thus can be used to determine the edge locations.

$$|AS(x,y)| = \sqrt{\left(\frac{\partial m}{\partial x}\right)^2 + \left(\frac{\partial m}{\partial y}\right)^2 + \left(\frac{\partial m}{\partial z}\right)^2} \quad \text{.....Equation 2}$$

where *m* = magnetic anomaly.

Upward Continuation (UC)

Upward continuation transforms the potential field measures on one surface to the field that would be measured on another surface farther from all sources. This transformation attenuates anomalies with respect to wavelength; the shorter the wavelength the greater the attenuation. This upward continuation tends to emphasize anomalies caused by deep sources at and to reduce of anomalies caused by shallow sources. *Oasis Montaj 7.2* use *equation 3* to make upward continuation transformation (Whitehead and Musselman, 2010).

$$L(r) = e^{-hr} \quad \text{.....Equation 3}$$

h = the distance, in ground units;
r = wavenumber (radians/ground unit).
note:
r = 2πk, where k is cycles/ground unit.

Subtraction Image

Subtraction image of airborne magnetic is an image which describes magnetic anomalies at certain depth or above. The image subtraction image is a result of simple grid/raster subtraction of RTP or AS image by their UC image at certain depth. Thus, for example if the UC image at 500m represents magnetic anomalies at 500 m or below, it means that the subtraction image represents magnetic anomalies at 500 m or above. In subtraction image, the upward continuation process is assumed as an ideal process. It means that the upward continuation image is 100% derived from certain depth or below.

Rotation-variant Template Matching (RTM)

Rotation-variant template matching (RTM) algorithm was applied to subtraction image both for RTP (RTPS) and AS (ASS). The first step to apply the method is determining region of interests (ROI's) to assign into template. The ROI's consist two areas which were considered as representatives of different lithologies. Van der Werff et al. (2007) explained that the template is a miniature image which consists of 3x1 pixels. The template contains information about a boundary between two contrast pixels. These two contrast pixels represent two different lithologies. This template is moved over the image like a moving kernel. At every position, the template is rotated, and a statistical fit is calculated for every pose (*Figure 6*).

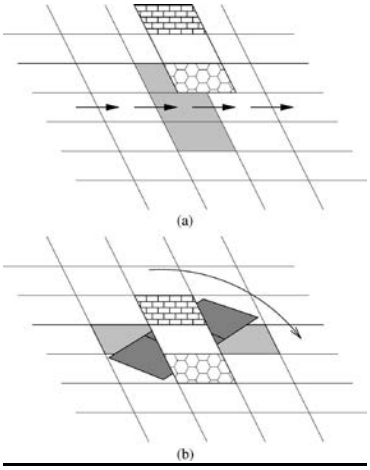


Figure 6 Template is matched by (a) moving it over an image and (b) changing the template orientation at every position by 45° increments up to a total of eight orientations (Van der Werff et al., 2007).

Clustering-based Edge Detection (CED)

Clustering-based edge detection (CED) algorithm from Dinh et al. (2009) for edge detection was applied to airborne magnetic data with some modifications. The algorithm consist 5 (five) steps with the first step as data preparation. In the first step, gaussian blur convolution was applied into subtraction image (RTPS or ASS). After the convolution, total horizontal derivatives were determined. The second step is applying *k-means*

clustering into total horizontal derivatives. Dinh et al. (2009) explained that 4 to 8 clusters can be tried as an input in k-means clustering in this step. Refining the clusters and distinguishing clusters into edge and non-edge cluster are becoming the next two steps. The last step is changing the threshold to refine the results. In this research, for practical reason, four clusters were taken as an input to determine edge and non-edge cluster. By determining only four clusters, it was easier to determine which ones is edge clusters without complex threshold determination process. Thus, the last step, threshold determination, could be skipped.

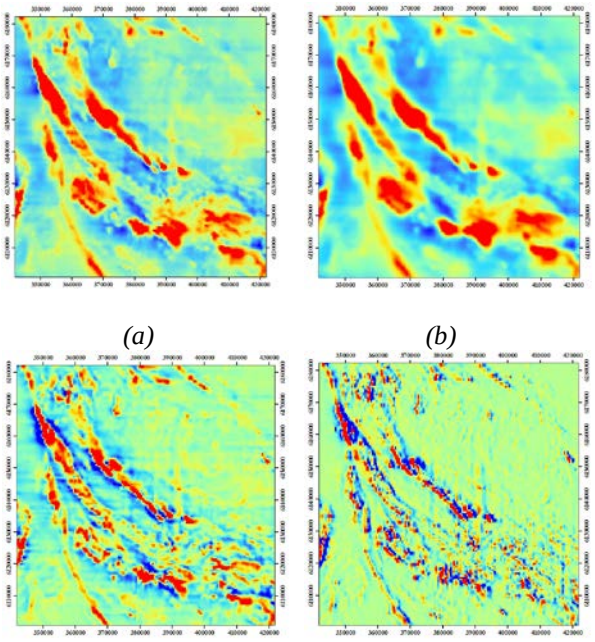
RESULTS AND DISCUSSION

Figure 7 show the results of data preparation process for RTP transformation part. *Figure 7(a)* is a result of RTP transformation with 20.3° and 74.9° for geomagnetic inclination and declination, respectively. The values of inclination and declination were generated by *Oasis Montaj 7.2* with latitude and longitude of the area as well as the time of data acquisition as the inputs. *Figure 7(b)* is a result of upward continuation of RTP image at 500 m. Furthermore, *figure 7(c)* is a result of subtraction between RTP and UP of RTP image. *Figure 7(d)* is horizontal derivates of subtraction images. Subtraction RTP and horizontal derivative of subtraction RTP image were used an input for template matching and k-means clustering technique, respectively. In addition, *figure 8* show the results for the same process but the first transformation that was applied is AS transformation not RTP.

Figures 9 show the results of RTM algorithm application to subtract image of RTP and AS, respectively. Both images have the same patterns except in the thickness of the lines. The RTP one has thicker lines than the AS one, it is might be because of threshold values differences. The threshold values were simply determined by natural break option in *ArcGIS 10*, the default option for classifying data. Thicker lines have a meaning that more pixels categorized as boundaries. Thus, if the lines are considered as the boundaries, then the RTP one has fuzzier boundaries than the AS one. It might be because the application RTP to the data is not effective. Milligan and Gunn (1997) explained that the transformation will effective for the areas above 15° and below 50° in latitude (study area latitude: 55°) whereas the AS transformation likely works well. After AS transformation, the peaks of analytic signal functions are symmetrical and occur over the edge of wide bodies (Milligan and Gunn, 1997). Consequently, the result of RTM with RTP would have more transitional areas than those of AS.

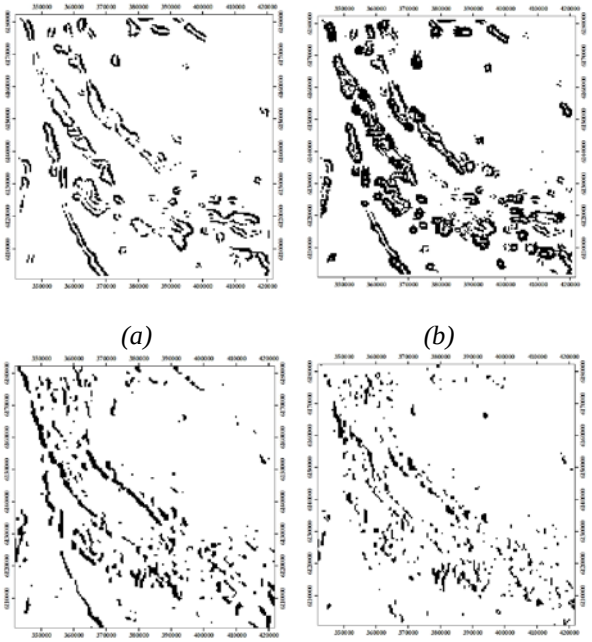
As can be seen in *figure 9*, the results of edge detection using *k-means* clustering for horizontal derivatives of subtract images both for RTP and AS are similar. Like RTM results, CED results show similarity pattern between RTP and AS except in the thickness of the lines. The RTP one have thicker and clearer lines than the AS one. Moreover, the lines lie on the flank of lithologies tends to be thicker.

The lines or edge clusters from both methods are not coinciding to lithology boundaries of existing map as shown in *figure 9*. However, most of edge clusters are accumulating within Hogem Batolith. Thus, Hogem Batholith could be distinguished to surrounding rocks. The new interpretation of lithology boundaries that separated Hogem Batholith with the surrounding lithologies base on the integration of four results can be seen in *figure 10*. Nelson et al. (1992) explained that prominent magnetic properties of Hogem Batholiths are caused by at least three phases of its formation. Each phase produced many textural and compositional variant that form complex features. Thus, to describe its complexity, Hogem Batholith is called as an intrusive complex.



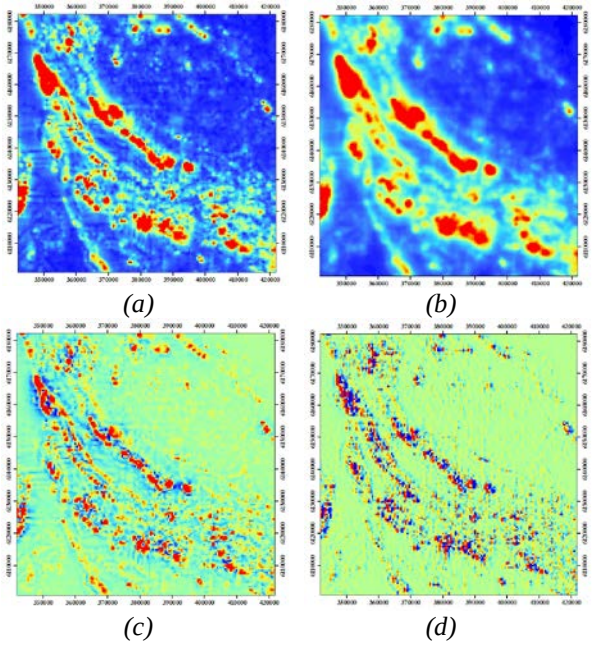
(a) (b) (c) (d)

Figure 7 Results of process for airborne magnetic filtering for Airborne magnetic; (a) reduce to Pole (RTP), I=20.3°, D=74.9°; (b) upward continuation RTP at 500 m (UC); (c) RTP Subtraction image (RTPS), RTPS=RTP-UC; (d) horizontal derivatives of RTP subtraction image



(a) (b) (c) (d)

Figure 8 Image of edge detection technique results, (a) an image result for RTM technique with RTP transformation, (b) an image result for RTM technique with AS transformation, (c) an image result for CED technique with RTP transformation, (d) an image result for CED technique with AS transformation.



(a) (b) (c) (d)

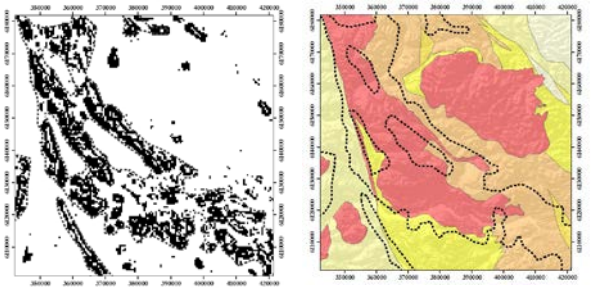


Figure 9 New interpretation of Hogem Batholith based on combination of two edge detection techniques results, RTM and CED.

CONCLUSIONS

RTP and AS transformation to airborne magnetic data at latitude more than 50° produced similar results in edge detection method. Edge detection method such as RTM and CED, could be applied to airborne magnetic data in order to help lithologic mapping by distinguishing intrusive complex rocks to surrounding rocks.

REFERENCES

Blakely, R.J. (1996), "Potential theory in gravity and magnetic applications", Cambridge, Cambridge University Press, 441 p.

Delong, R.C. (1996), "Geology, Alteration, Mineralization and Metal Zonation of the Mt. Millihan Porphyry Copper-Gold Deposits", Vancouver, The University of British Columbia.

Dinh, V., Leitner, R., Paclik, P., and Duin, R. (2009), "A Clustering Based Method for Edge Detection in Hyperspectral Images", *in* Salberg, A.-B., Hardeberg, J., and Jenssen, R., eds., Image Analysis, Volume 5575: *Lecture Notes in Computer Science*, Springer Berlin / Heidelberg, p. 580-587.

Massey, N.W.D., MacIntyre, D.G., Desjardins, P.J., and Cooney, R.T. (2005a), "Digital Geology Map of British Columbia - Tile NN10 Central B.C.", *GeoFile 2005-6*, B.C. Ministry of Energy and Mines.

Massey, N.W.D., MacIntyre, D.G., Desjardins, P.J., and Cooney, R.T. (2005b), "Digital Geology Map of British Columbia: Tile NO10 Northeast B.C", *GeoFile 2005-10*, B.C. Ministry of Energy and Mines.

Massey, N.W.D., MacIntyre, D.G., Desjardins, P.J., and Cooney, R.T. (2005c), "Digital Geology Map of British Columbia:Tile NO9 North Central B.C.", *GeoFile 2005-9*, B.C. Ministry of Energy and Mines.

Massey, N.W.D., MacIntyre, D.G., Haggart, J.W., Desjardins, P.J., Wagner, C.L., and Cooney, R.T. (2005d), "Digital Geology Map of British Columbia: Tile NN8-9 North Coast and Queen Charlotte Islands/Haida Gwaii", *GeoFile 2005-5*, B.C. Ministry of Energy and Mines.

Milligan, P.R., and Gunn, P.J. (1997), "Enhancement and Presentation of Airborne Geophysical Data", *Journal of Geology and Geophysics*, **v. 17**, p. 63-75.

Natural Resources Canada (2010), "Geoscience Data Repository, Aeromagnetic and Electromagnetic data", Natural Resources Canada, http://gdr.nrcan.gc.ca/aeromag/index_e.php.

Nelson, J., Bellefontaine, K., Rees, C., and MacLean, M. (1992), "Regional Geological Mapping in the Nation Lakes Area (93N/2E,7E), *Geological Field Work 1991", Paper 1992-1*, British Columbia Ministry of Energy, Mines and Petroleum Resources, p. 118.

Nelson, J., Bellefontaine, K.,Green, K., and MacLean, M. (1991), "Regional Geological Mapping Near the Mount Milligan Deposit (93N/l,93k/16)", *Geological Fieldwork 1990, Paper 1991-1*, British Columbia Ministry of Energy, Mines and Petroleum Resources.

R Core Team (2013), "R: A language and environment for statistical computing", R Foundation for Statistical Computing, Vienna, Austria, http://www.R-project.org/.

Roest, W.R., Verhoef, V., and Pilkington, M. (1992), "Magnetic interpretation using the 3-D analytic signal", *Geophysics*, **v. 57**, p. 116-125.

Van der Werff, H., Van Ruitenbeek, H., Van der Meijde, M., Van der Meer, F., Jong, S.d., and Kalubandara, S. (2007), "Rotation-Variant Template Matching for Supervised Hyperspectral Boundary Detection", *IEEE Geoscience and Remote Sensing Letters*, **v. 4**, p. 70-74.

Whitehead, N., and Musselman, C. (2010), "montaj MAGMAP Filtering:2D Frequency Domain Processing of Potential Field Data Extension for Oasis montaj v7.1", *Tutorial and User Guide*, Ontario, Geosoft Inc., 73 p.